SIMULATION AND OPTIMIZATION OF A GREENHOUSE-TYPE SOLAR DRYER WITH COMSOL MULTIPHYSICS

Abstract

Solar drying remains for developing African countries the only economical means of preserving foodstuffs for which post-harvest losses sometimes reach 60%. Improvement of design methods for solar dryers operating in direct mode with natural convection have been carried out, but not enough efficiently. This study allowed to model the different elements that compose a greenhouse drying system by natural convection, using a system of non-linear and strongly coupled partial differential equations, based on the heat, matter and momentum balances between the different exchange media. The resolution of this system of equations was carried out by the finite element method (with the COMSOL software), thus allowing to simulate the operation of a greenhouse solar dryer. This mathematical model was used to describe the dynamic behavior and heating value of greenhouse-type solar dryers. The optimization study through simulations also made it possible to compare the drying power of more than 180 solar dryers. Analysis of simulation results gave the dryer of small size (height= 2.5 m and width = 3 m) with large identical openings (width inlet = width outlet = 25 cm) positioned at both extremes: bottom for inlet (Yi = 0.1 m) and high for the air outlet (Yo = 1.65 m), as an dryer optimized and efficient in energy (Tm = 50.73 °C). The average air speed (Vm = 0.58 m. s^{-1}) in this dryer is also remarkable and could be used for drying all food products.

Keywords: Greenhouse solar dryer; Heat transfer; Energy and mass balance; modeling; optimization; simulation.

Nomenclature

ϱ : Density (kg/m^3)

Cp :Heat capacity at constant pressure J/ (kg.K)

k : Thermal conductivity W/(m.K)

q : Heat source or volume density of energy generated (w/m^3)

***ε*:** Coefficient of emission

G : Irradiation from a surface (W/m^2)

σ: Stefan's constant ($W.m^{-2}.K^{-4}$)

he : Heat transfer coefficient of outside air ($W.m^{-2}.K$)

T : Temperature (K)

x: Space variable in the horizontal direction (m)

y : Space variable in the vertical direction (m)

u : Air velocity in the dryer according x (m/s)

v: Air velocity in the dryer according y (m/s)

t : Time (h)

η : Dynamic viscosity of the fluid (air) (Pa.s).

ξ : elongational viscosity (Pa.s)

Y : Open position (m)

l : Opening size (m)

clues

lamp : lamp

air : air

s : exit

e : entry

amb : ambient

0 ; i : initial

1. INTRODUCTION

Drying is an important operation in the agro-food and agro-industrial sector. This operation, which consists of partially or totally removing water from a wet product, constitutes a means of conservation (stabilization) or a stage in the processing of certain products [1-4]. However, the procedure is still archaic or very expensive, especially for developing countries where electricity is hardly accessible. Added to this, are soaring prices and the shortage of fuels used as a source of energy. These reasons have spurred various studies and deep research on the use of solar energy as an alternative energy source, particularly in developing countries [5]. Indeed, in these countries, although the amount of sunshine is high throughout the year, the use of traditional methods continues to prevail. Added to this are all the constraints related to traditional drying. The drying operation must be carried out by optimizing the amount of heat needed to obtain a quality product with a minimum overall energy expenditure in order to minimize the loss not only in terms of quantity but also in terms of the quality of the dried product.

Although it observed a marked increase in research on solar dryers, the effort remains modest compared to the complexity, diversity and size of the problem. It is therefore not surprising that most solar dryers developed are neither efficient nor accepted by their intended users. This poor performance is mainly explained by the discrepancy that is usually found between the working temperature and the flow rate of the air circulating in the dryers [6]. Low popularity among farmers is usually related to the cost of the drying system as well as social barriers ignored or overlooked at the design stage. Work published generally deals only with the construction of the works and often omits data which would allow the dryer to be improved or adapted to another location or to another agricultural product. There is also a lack of basic data on the operation of solar dryers with natural air circulation [6] . This work is therefore in line with the objective of improving and optimizing the sizing and design methods of solar dryers, with a focus on the use of digital simulation tools like Comsol Multiphysics 4.0 software. This study is based on a mathematical model describing dynamic behavior and calorific value of several greenhouse type solar dryers. This helps to retain the optimal structure that can adapt to a given environment and product.

Methodology

2.1 Description of solar dryer selected

In order to facilitate its construction and make it accessible to farmers, we opted for a classic and fairly simple dryer model. It is a direct solar dryer for agricultural purposes intended for the drying of agricultural products such as cocoa and possibly for their storage in bags. The device on the characteristics of which we have elaborated our model is presented in Fig.1.

Fig. 1. Basic structure of the greenhouse type dryer used in the study.

The structure set up is a greenhouse; it respects the recommendations concerning the orientation of greenhouse [7], namely:

- Two kinds of openings (air inlet and outlet) on the lateral walls perpendicular to the North-South direction.
- The air inlets are at the level of the wall receiving the prevailing wind: north-south direction and the exit on the opposite wall.
- The long axis of the greenhouse is parallel to the east-west direction.

Sidewalls and sensors are in glass except for the west surface which is clear plastic. The inclination of the sensors is 18 degrees to the horizontal.

2.2 Equation setting

The equation was made using a simplified diagram of the basic device of the dryer.
The mathematical modeling of transfers and fluid behavior within the dryer can be established from energy balances and momentum reflecting energy conservation and fluid dynamics.
For the sake of simplification, the proposed model is based on the following assumptions:

- The geometric and physical properties of the greenhouse are assumed to be uniform in the direction of its long axis.
- The greenhouse is thus assimilated to its transverse cross section and the edge effects linked to the ends are neglected.
- The cover of the greenhouse is considered as a thin thickness surface where the conductive exchange between the outer and inner faces can be neglected.
- Solar radiation captured by the side faces of the greenhouse is neglected.
- The sun here is represented by a radiative lamp thus with permanent radiation.

The above-mentioned hypotheses allow the simplified schematization (Fig. 2.) of the solar dryer and the thermal transfers involved.

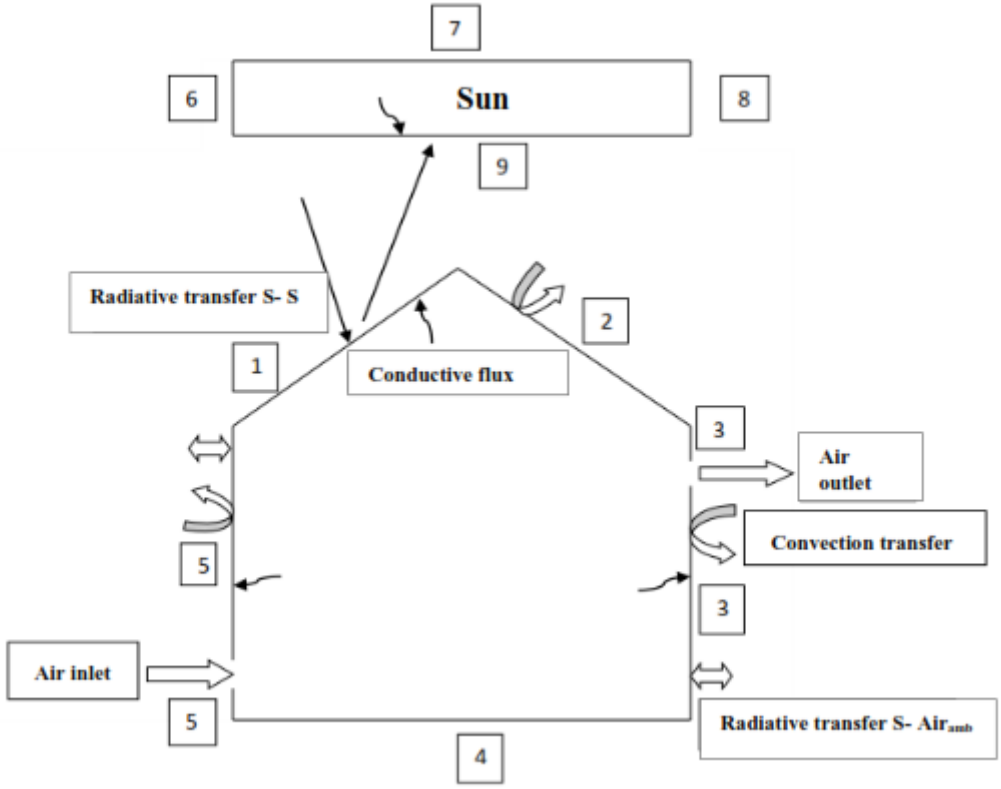

Fig .2. Elements and mechanisms to be considered in a solar dryer model

2.3 Systems of equations

The system of equations describing the conservation of energy, the continuity and the transport of momentum for the sub-domains and limits of the solar dryer is written like this:

2.3.1 Energy conservation equations and boundary conditions

These equations are obtained by applying conservation law of energy at the level of subdomains as well as their different limits.

- Subdomain II (sun)

$$\varrho_{lamp}\, Cp_{lamp} \frac{\partial T_{II}}{\partial t} - k_{lamp}\left(\frac{\partial^2 T_{II}}{\partial x^2} + \frac{\partial^2 T_{II}}{\partial y^2}\right) = q_{lamp} \qquad (2.1)$$

With $0 \leq y \leq e_{lamp} = 0{,}5$ *m or 1 m and* $0 \leq x \leq 3$ *m or 6 m* for the subdomain II.

- Limits of the subdomain II

Limit 9

$$-k_{lamp}\left(\frac{\partial T_9}{\partial y}\right) = \varepsilon\,(G - \sigma T_9^{\,4}) \qquad (2.2)$$

With $0 \leq y \leq e_{lamp} = 0{,}5$ *m or 1 m for this limit*

Limits 6, 7et 8

$T = T_0$ (2.3)

- Subdomain I (drying chamber)

$$\varrho_{air}\, Cp_{air} \frac{\partial T_I}{\partial t} - k_{air}\left(\frac{\partial^2 T_I}{\partial x^2} + \frac{\partial^2 T_I}{\partial y^2}\right) = 0 \quad (2.4)$$

With $0 \leq x \leq$ 3 m or 6 m ; $0 \leq y \leq$ 2,5 m or 5 m for this subdomain

- Limits of the subdomain I

Limits 1 et 2

$$-K_{air}\cos\beta\left(\frac{\partial T_1}{\partial x}\right) + K_{air}\sin\beta\left(\frac{\partial T_1}{\partial y}\right) = he\,(T_0 - T_1) + \varepsilon\,(G - \sigma T_1^4) \quad (2.5)$$

$$K_{air}\cos\beta\left(\frac{\partial T_2}{\partial x}\right) + K_{air}\sin\beta\left(\frac{\partial T_2}{\partial y}\right) = he\,(T_0 - T_2) + \varepsilon\,(G - \sigma T_2^4) \quad (2.6)$$

For these limits, because of the inclination of an angle β, we have:

$0 \leq y \leq$ 0,5 m or 1m et $0 \leq x \leq$ 3 m or 6 m and $\beta = \pi/10$

Limits 3, 5, 3'et 5'

$$-K_{air}\left(\frac{\partial T_3}{\partial x}\right) = he\,(T_0 - T_3) + \varepsilon\sigma(T^4_{amb} - T_3^4) \quad (2.7)$$

$$-K_{air}\left(\frac{\partial T_5}{\partial x}\right) = he\,(T_0 - T_5) + \varepsilon\sigma(T^4_{amb} - T_5^4) \quad (2.8)$$

$$-K_{air}\left(\frac{\partial T_{3'}}{\partial x}\right) = he\,(T_0 - T_{3'}) + \varepsilon\sigma(T^4_{amb} - T_{3'}^4) \quad (2.9)$$

$$-K_{air}\left(\frac{\partial T_{5'}}{\partial x}\right) = he\,(T_0 - T_{5'}) + \varepsilon\sigma(T^4_{amb} - T_{5'}^4) \quad (2.10)$$

For these limits, we have: $0 \leq x \leq$ 3 m or 6 m

Limit 4

$$K_{air}\left(\frac{\partial T_4}{\partial y}\right) = 0 \quad (2.11)$$

For this limit, we have : $0 \leq y \leq$ 2,5 m or 5 m

Air outlet and air inlet limit

$$\frac{\partial T_s}{\partial x} = 0 \quad et \quad T_e = T_0 \quad (2.12)$$

For the output limit, we have: $0 \leq x \leq$ 0,002 m

2.3.2 Equations of continuity, transport of momentum and boundary conditions

- Subdomain I

We have u = (*u*, *v*) so:

$$\frac{\partial \varrho_{air}}{\partial t} + \varrho_{air}\left(\frac{\partial u}{\partial x} + \frac{\partial v}{\partial y}\right) + u\frac{\partial \varrho_{air}}{\partial x} + v\frac{\partial \varrho_{air}}{\partial y} = 0 \quad (2.13)$$

$$\left\{ \varrho_{air}\frac{\partial u}{\partial x} + \varrho_{air}\, u\frac{\partial u}{\partial x} + \varrho_{air}\, v\frac{\partial u}{\partial y} = 2\eta\left(\frac{\partial^2 u}{\partial x^2} + \frac{\partial^2 u}{\partial y^2}\right) + \left(\xi - \frac{2}{3}\eta\right)\left(\frac{\partial^2 u}{\partial x^2} + \frac{\partial^2 v}{\partial x \partial y}\right) + F_x \quad (2.14)$$

$$\varrho_{air}\frac{\partial v}{\partial x} + \varrho_{air}\,u\frac{\partial v}{\partial x} + \varrho_{air}\,v\frac{\partial v}{\partial y} = 2\eta\left(\frac{\partial^2 v}{\partial x^2} + \frac{\partial^2 v}{\partial y^2}\right) + \left(\xi - \frac{2}{3}\eta\right)\left(\frac{\partial^2 v}{\partial y^2} + \frac{\partial^2 u}{\partial x \partial y}\right) + F_y$$

With $F_y = g(\varrho_{air0} - \varrho_{air})$, $F_x = \xi = 0$ and P = cte and with $0 \leq x \leq 3\ m$ or $6\ m$;

$0 \leq y \leq 2{,}5\ m$ or $5\ m$ *for this subdomain* I

- Limits of the subdomain I

  Limits 1, 2, 3, 4, 5, 3'et 5'

  We have u = (*u, v*)=0 (2.15)

  Air inlet limit

We have u= $u_e = U_0$ (2.16)

Air outlet limit

$$\frac{\partial \varrho_{s_{air}}}{\partial t} + \varrho_{s_{air}}\left(\frac{\partial u_s}{\partial x} + \frac{\partial v_s}{\partial y}\right) + u_s\frac{\partial \varrho_{s_{air}}}{\partial x} + v_s\frac{\partial \varrho_{s_{air}}}{\partial y} = 0 \quad (2.17)$$

$$\begin{cases} \varrho_{s_{air}}\frac{\partial u_s}{\partial t} + \varrho_{s_{air}}u_s\frac{\partial u_s}{\partial x} + \varrho_{s_{air}}v_s\frac{\partial u_s}{\partial y} = 0 \\ \varrho_{s_{air}}\frac{\partial v_s}{\partial t} + \varrho_{s_{air}}u_s\frac{\partial v_s}{\partial x} + \varrho_{s_{air}}v_s\frac{\partial v_s}{\partial y} = g(\varrho_{air0} - \varrho_{s_{air}}) \end{cases} \quad (2.18)$$

With $0 \leq x \leq 0{,}002\ m$ and $0 \leq y \leq 25$ cm or 50cm for this limit

2.3.3 Initial conditions

- Initial conditions of Subdomain II (sun)

  At, t = 0 the subdomain II is assumed at the temperature T = T_0 external temperature.

- Initial condition of Subdomain I (Drying chamber)

  In this subdomain, the initial condition is as follows: at t = 0 the air is considered at the temperature T = T_0.

2.4 Digital resolution

The development of the system of equations gives nonlinear partial differential equations in U, ρ and T; solved with the Comsol Multiphysics 4.0 software by the finite element method (FEM).

Since 1969 the FEM has been known as a general tool for solving partial differential equations (PDE), and is used to solve non-linear and non-stationary problems in several domains [8-9].

The steps for applying the finite element method are as follows [8]; [10-11]:

• 1st stage: the rewriting of the equations in integral form followed by a weak formulation to include the boundary conditions.

• 2nd stage: the preparation of geometric data which consists of discretizing the domains into elements and calculating the connectivities of each as well as the coordinates of its nodes.

• 3rd stage: the construction of elementary matrices; in this step the variables of each element are approximated by simple linear, polynomial or other functions. The degree of the interpolation polynomial is related to the number of nodes of the element.

Note that the nodal approximation is appropriate.

• 4th stage: all the properties of the elements must be assembled to form the algebraic system for the nodal values of the physical variables. It is at this level that the connectivities calculated in stage 2 are used to construct the global matrices from the elementary matrices.

2.5 Drying optimization studies under COMSOL

The optimization study involved three aspects. The first one is the determining of dryer optimum size by using two simulations with two dryers of different sizes (fig.3.).

The second aspect concern the determination of optimal opening positions (fig .4.) air inlet and outlet). Thus, several simulations were performed by varying the positions from top to bottom from the extreme positions: 0.1 m (low) and 1.9 m or 3.9 m (high) depending on the size.

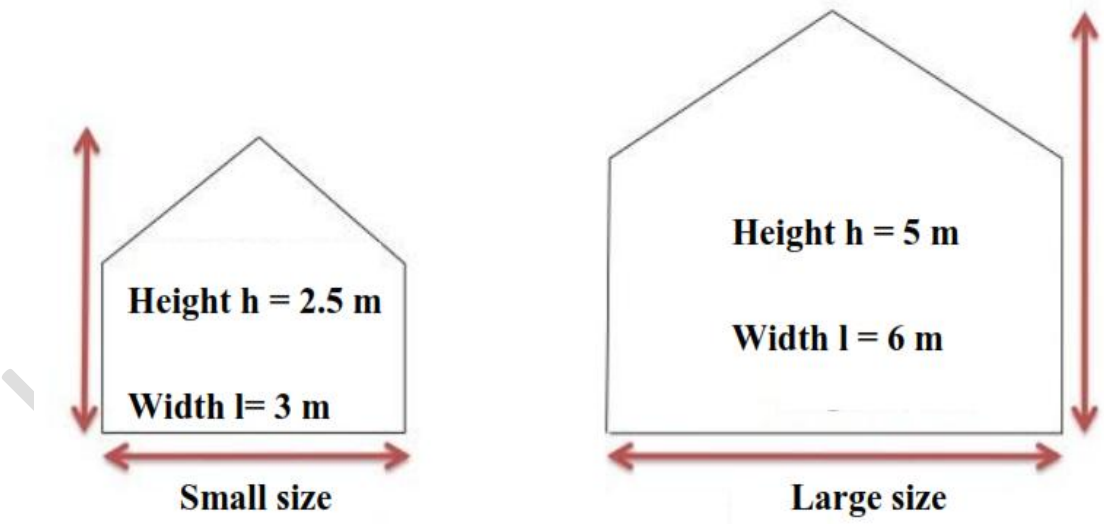

Fig .3. Characteristics of the two types of greenhouse dryers to be optimized

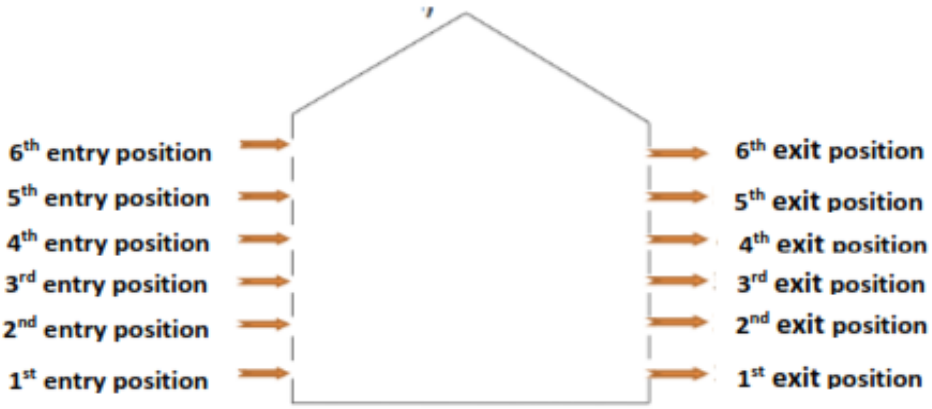

Fig .4. Different positions of air entry and exit, simulated successively, on the greenhouse dryer.

The third aspect concerning the determination of optimal dimensions (air inlet and outlet). Several simulations were carried out by varying the dimensions from 5 cm to 25 cm in steps of 5 cm; this is five (5) dimensions in total. The last two aspects of the optimization study led to 180 situations or scenarios in total, therefore 180 simulated driers for each dryer size. Recall that a size, positions and dimensions of openings are said to be optimal if and only if the average pair of parameters (temperature, velocity) of air within the dryer is the highest possible.

2.6 Presentation of different situations or scenarios

Several scenarios are characterized by a fixed input position corresponding to an output position that is likely to vary. Thus, for example, when the input is fixed as shown in fig .5.

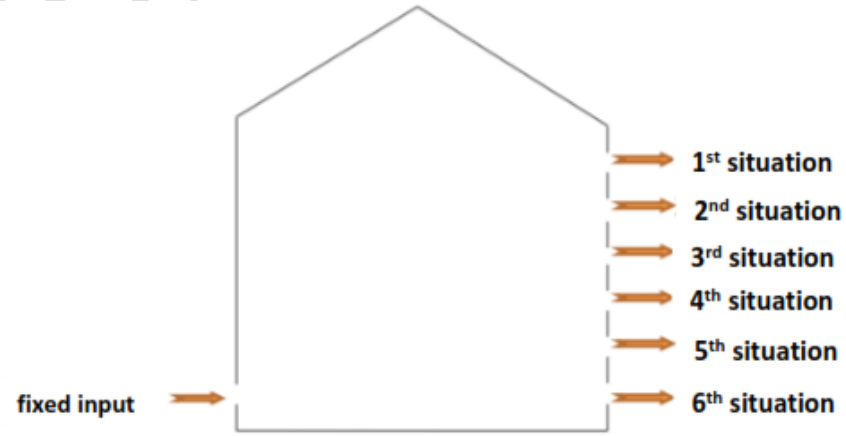

Fig .5. The different situations possible for a fixed air input

There are six (6) possible output positions corresponding to this fixed input position therefore six (6) situations for this input position. Since we have six (6) input positions, this leads to 36 situations or scenarios for these six (6) positions and since we have 5 opening dimensions, this makes 180 situations in total. Recall that the intervals observed for each opening position according to the opening dimensions are as follows:

- 0,35 m for the dimensions: l_{entry} = 5 cm and l_{exit} = 5 cm
- 0,34 m for the dimensions: l_{entry} = 10 cm and l_{exit} = 10 cm
- 0,33 m for the dimensions: l_{entry} = 15 cm and l_{exit} = 15 cm
- 0,32 m for the dimensions: l_{entry} = 20 cm and l_{exit} = 20 cm
- 0,31 m for the dimensions: l_{entry} = 25 cm and l_{exit} = 25 cm

2.7 Influence of the dimensions of openings on the temperature and the speed of the air

The influence of the opening dimensions on the temperature and air velocity within the dryer, will be from the optimal positions and opening dimensions that will be obtained. It will be to fix a dimension (input or output) from the optimal and to vary the other. Recall that five (5) dimensions or variations (5 cm, 10 cm, 15 cm, 20 cm and 25 cm) were necessary.

3. RESULTS AND DISCUSSION

3.1 Results

3.1.1 Optimal size of the dryer

The simulation results to determine the optimal size of the solar dryer are shown in Fig .6, 7 and 8. Depending on the size of the dryer, there are differences in internal temperature and air fields velocity.

3.1.1.1 Internal temperature distribution

Analysis of Fig .6. shows an overlap of five color bands (red, yellow, green, blue, and indigo) indicating the temperature distribution at the two types of dryers, after 10 hours of simulation; the bands are wider on the small dryer than on the large. This would mean that the small dryer is energy efficient compared to the large one.

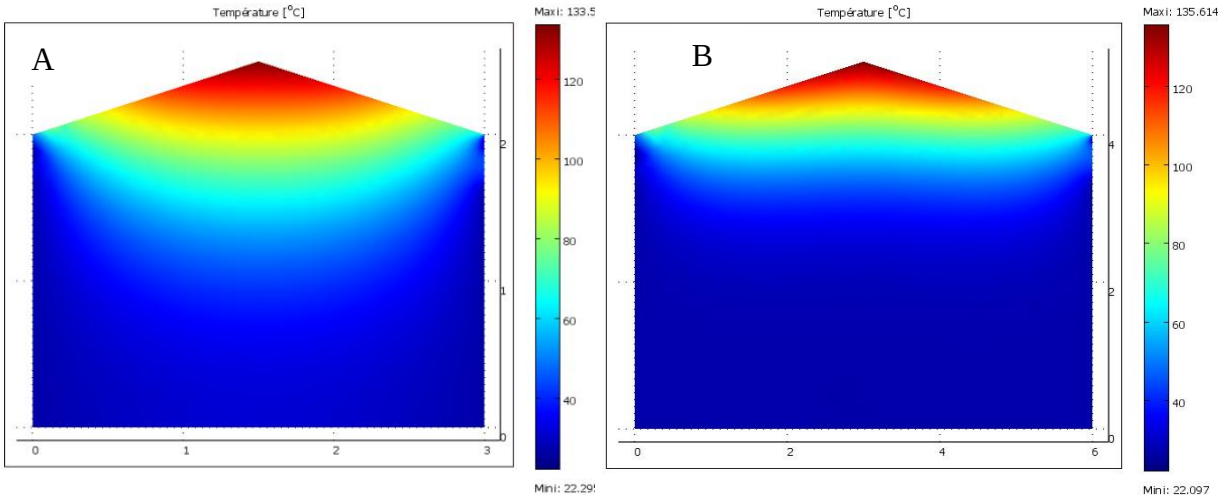

Fig.6. Internals temperatures distribution in the small (A) and large (B) dryer

This energy performance is confirmed by Figure 7 giving the temperature profiles after 10 hours of simulation.

In Fig .7, we can see that the temperature profile of the small dryer is much higher than that of the large dryer with an average temperature of 39.46°C versus 34.74°C. This represents a difference of 4.72 °C, not negligible.

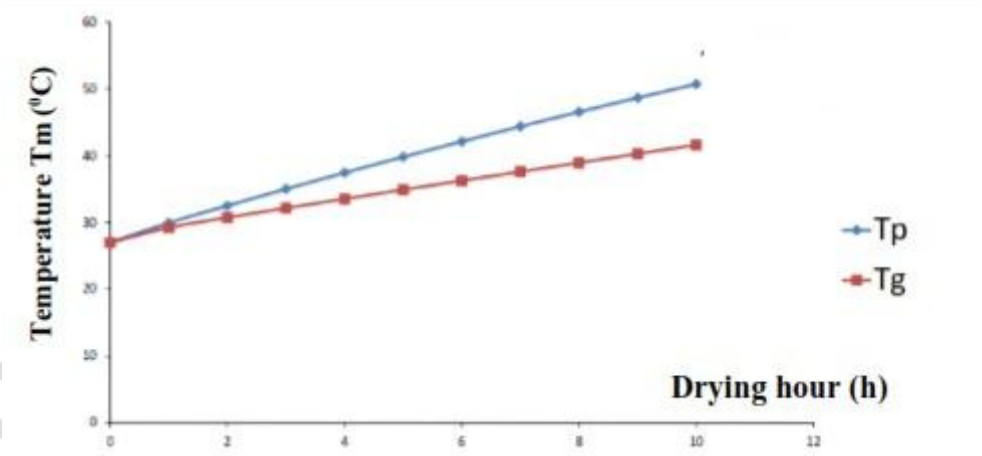

Fig .7. Temperature profile of the small dryer (Tp) and the large dryer (Tg) after 10 h of functioning

3.1.1.2 Internal velocity fields

Analysis of Fig .8. shows an intermingling of three (3) colors (green, blue and indigo); the green color representing large velocity values is much more visible in the small dryer. This would mean that this dryer is more fluid in terms of air movement. This fluidity is confirmed by the value of the average velocity after 10 hours of simulation with a value of 0.58 m/s against 0.33 m/s for the large dryer.

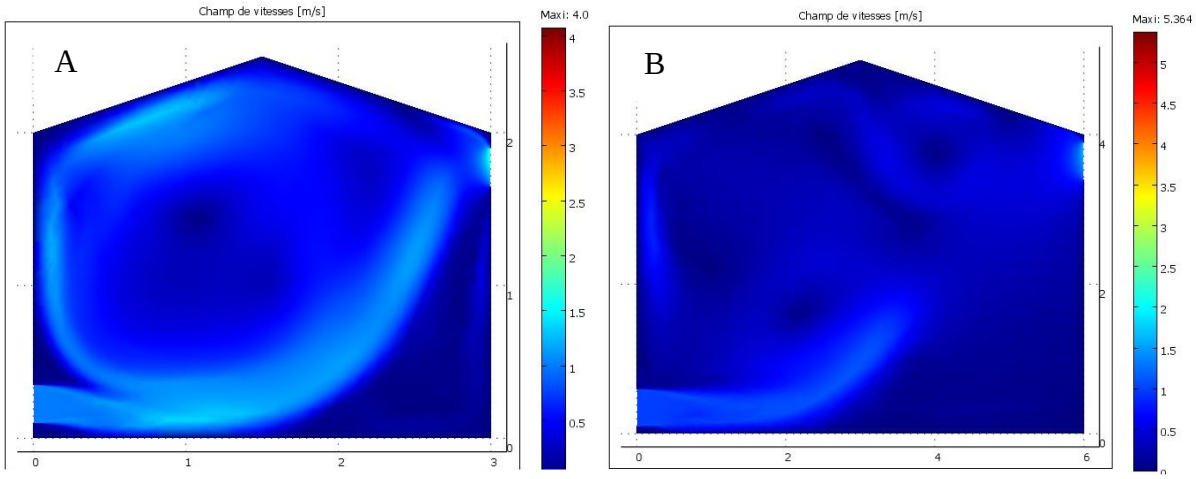

Small dryer : **Vm=0.58 m/s** at t= 10 h

Large dryer : **Vm=0.33 m/s** at t= 10 h

Fig .8. Internal velocity fields in the small (A) and the large (B) dryer

3.1.2 Optimal positions and dimensions of dryer opening for air inlet and outlet

All these results combine to say that the small dryer is the most efficient; thus, the continuation of the optimization study concerned this type of dryer. With dimensions and extreme positions as shown in Fig .9.

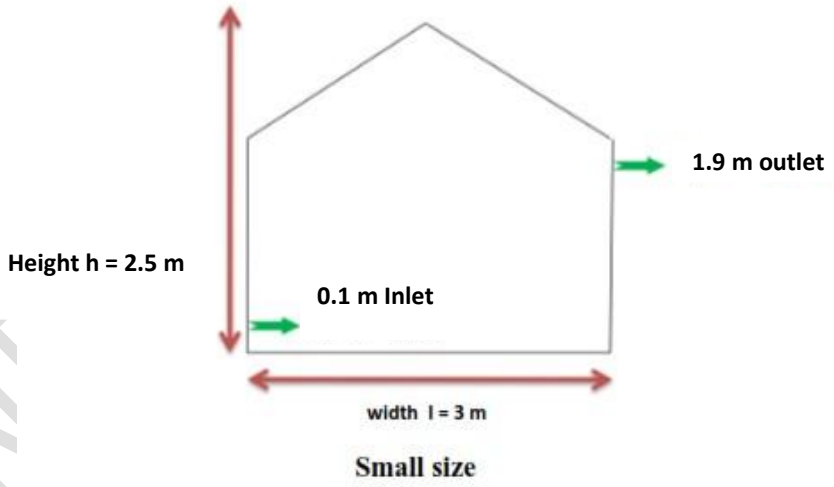

Fig .9. Characteristic of small dryer optimized: air inlet and outlet position on the dryer

Simulation results to determine the optimal opening dimensions and positions of the solar dryer are presented by the curves (Fig .10 and 11). It is recalled that six (6) series of six (6) situations therefore 36 situations per dimension were performed. The evolution of the mean temperatures and air velocities within the dryer according to the different situations after 10 hours of simulation for each dimension of openings gives fig .10 and 11.

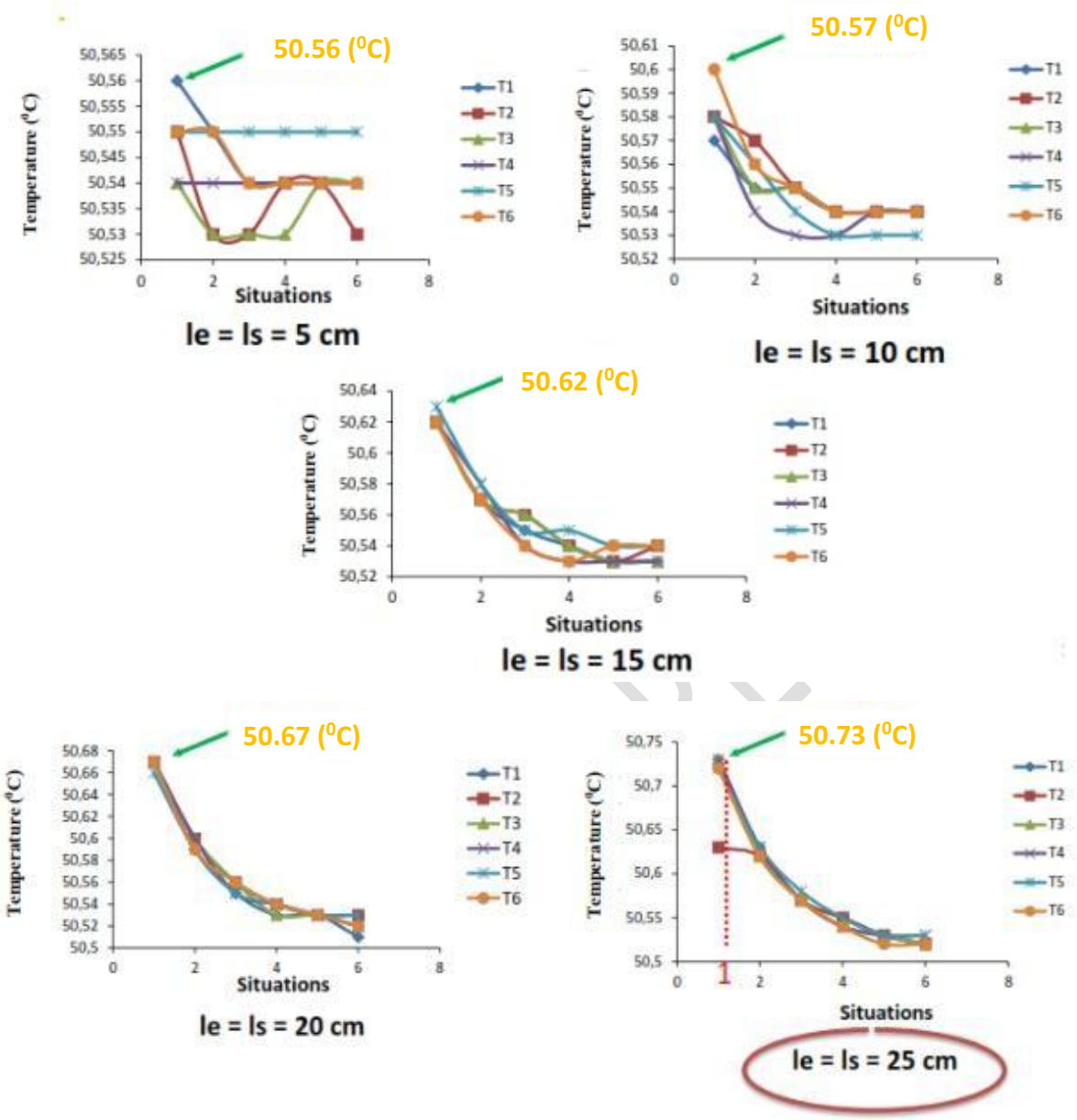

Fig .10. Evolution of the average air temperature according to the situations for each dimension (dryer opening): average temperature (Tm) at t = 10 h of simulation. le = entry width; ls = exit width

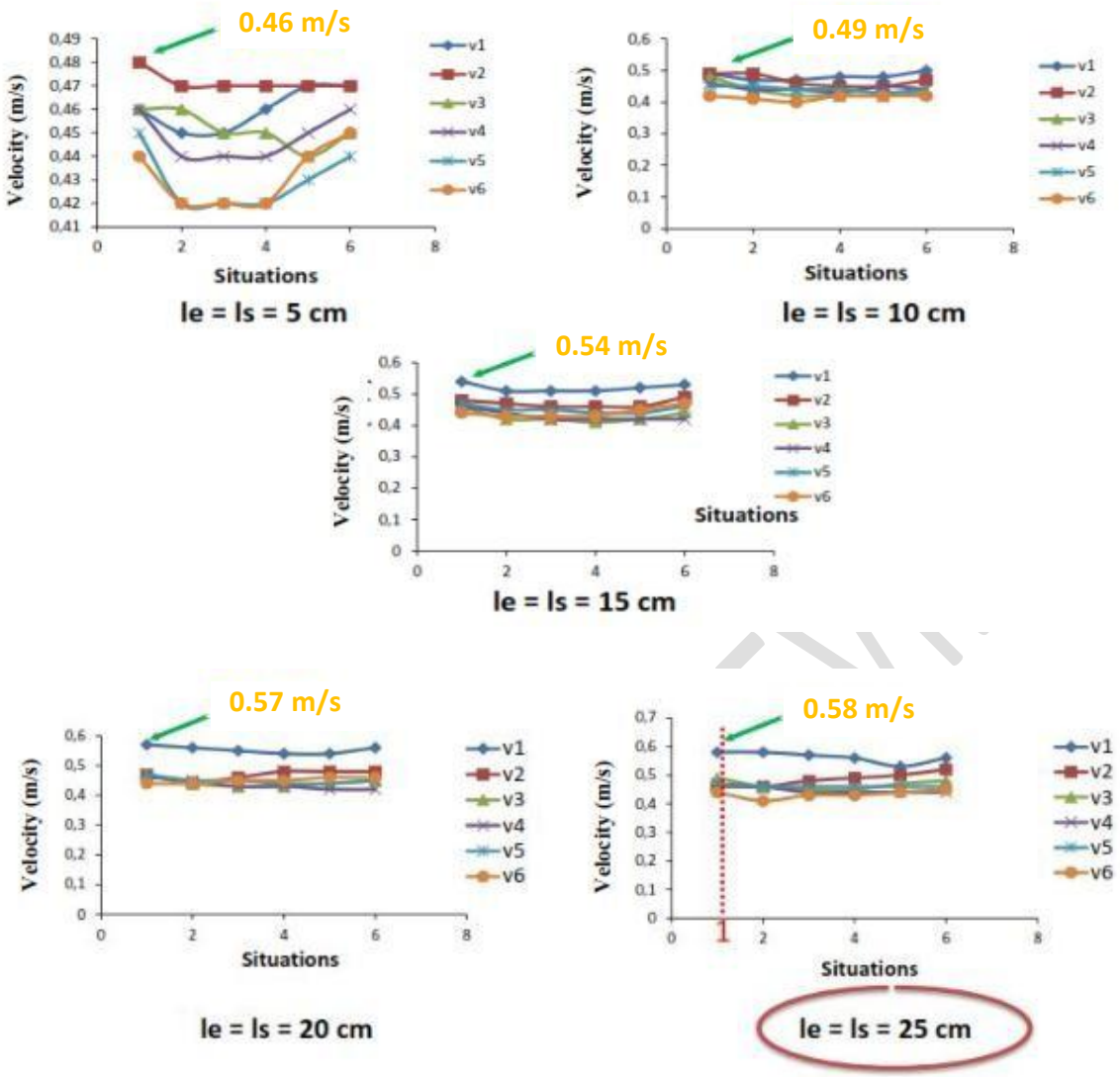

Fig .11. Evolution of the average air velocity according to the situations for each dimension (dryer opening): average velocity (Vm) at t = 10 h of simulation**.** le = entry width; ls = exit width

The analysis in Fig .10. shows that the curves vary very little according to the situations for each dimension of opening; the greatest values of temperatures are generally obtained at the level of the first situations of the first series. The largest value is obtained for large openings (le = ls = 25 cm) in the first situation of the first series. These observations are valid for Fig .11. The positions and optimal opening dimensions are thus obtained in the case of large openings (le = ls = 25 cm) and extreme positions (Ye = 0.1 m and Ys = 1.65 m) because this situation gives the large average values of the couple (temperature, velocity) of air within the dryer.

The values obtained for this situation are 50.73 ^{0}C and 0.58 m/s respectively for the average temperature and velocity at t = 10 h of simulation.

Recall that the curves (T1, T2, T3, T4, T5 and T6) and (V1, V2, V3, V4, V5 and V6) respectively represent the curves of the average temperature and velocity of the first series to the sixth. The series correspond to the six (6) specific air inlet positions.

3.1.3 Influence of the dimensions of openings on the temperature and the velocity of the air

The evaluation of the influence of the dimensions will be made starting from the positions and dimensions of optimal openings respectively (Ye = 0.1 m and Ys = 1.65 m) and (le = 25 cm and ls = 25 cm) by fixing either the air inlet or outlet.

The different cases below (Fig .12.) present the evolution of average temperatures (Tm) and velocities (Vm) of the air, at t = 10 h of simulation according to the 5 variations (5 cm, 10 cm, 15 cm, 20 cm and 25 cm) for each fixed dimension.

- Influence of the mean temperature (Tm) at t = 10 h of simulation

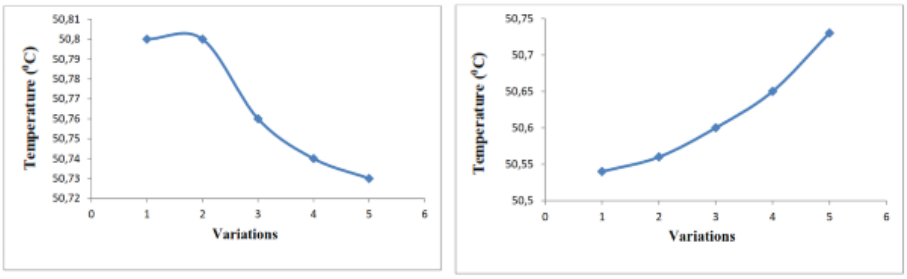

Case 1: exit fixed at 25 cm **Case 2**: entry fixed at 25 cm

- Influence of mean velocity (Vm) at t = 10 h of simulation

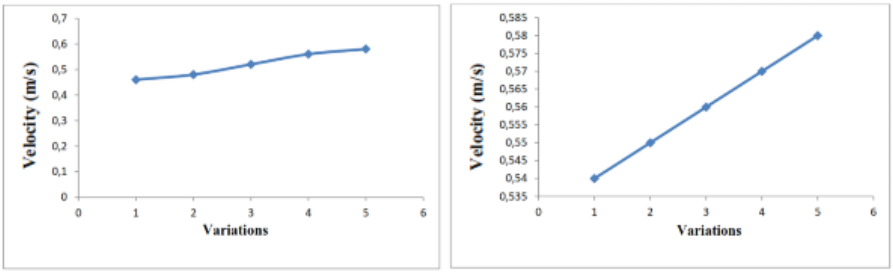

Case 1: exit fixed at 25 cm **Case 2**: entry fixed at 25 cm

Fig .12. Evolution of the average air velocity according to the 5 variations of dimensions for each fixed dimension.

The analysis of Fig .12. shows that a variation of one dimension by fixing the other from the optimal positions, causes a change in temperature and air velocity. Indeed, the temperature decreases while the velocity increases when the size of the input increases gradually with fixation of the output. When the output size increases gradually with fixation of the input, the temperature and velocity are slightly increased. We also note that the latest variations (for input and output) have the highest couple values (temperature, velocity). For these variations, it should be noted that we have le = ls = 25 cm the largest dimension value.

3.1.4 Statistical analysis of results

Student tests were carried out at the 5% threshold to assess the significance of the variations in temperature and air speed; when varying the positions and sizes of openings.

For convenience, these variations have been made based on optimal opening sizes and positions.

It is a question of comparing through these tests two series of average data for the temperature and for the speed of the air.

Table 1. Table of Student's test on temperature and air velocity when varying the opening positions of the dryer

Parameter Types	**F_{cal}**	**F_{lu}**	**C_{obs}**	**C_{lu}**
Temperature	56465.64	5.05	25.13	2.015
velocity	38.46	5.05	88.11	2.015

Table 2. Student test table on temperature and air velocity when varying the opening dimensions of the dryer

Parameter Types	**F_{cal}**	**F_{lu}**	**C_{obs}**	**C_{lu}**
Temperature	29.14	6.39	56.57	2.78
velocity	108.16	6.39	34.24	2.78

According to the tables, the criteria C_{obs} calculated from the data are higher than the critical values C_{lu} for the two parameters. Fisher's F calculated F_{cal} are also higher than the F_{lu} critical values.

There is therefore a significant difference between the dispersions and the means of the two sets of data concerning these parameters.

3.2 DISCUSSION

The results of temperature distribution and velocity fields at the level of the two dryers showed that the small dryers are the most efficient. Indeed, they have a significant energy power because they heat more and have a remarkable fluidity of air.

The significant energy power of small dryers can be explained by the short distances between the different limits. Indeed, the dominant process of heat transfer within the air as a homogeneous and isotropic medium assumed to be opaque is conduction. The transmission of heat from one limit to another is therefore strongly dependent on the distance which separates them according to Fourier's law. The exchange between two limits in the case of conduction is all the more rapid (high flux density) as the distance which separates them is small and slower for a greater distance according to the theory of conduction [12].

The significant air fluidity in the case of small dryers can be explained by the significant variation of the Archimedes force (volumic force) which is all the greater as the temperature is high. Indeed, the Archimedes force is the main instigator of the phenomenon of natural convection according to the principle of natural convection. [13].

The results obtained (Figures 6 and 8) can also find their explanations, by the slowness of the phenomenon of natural convection to be implemented in the case of the large dryer. This slowness can be explained by the large amount of air in large dryers [14].

The results relating to the determination of the optimal dimensions and positions of openings, show that for a dryer to have a high fluidity of air, it is necessary that the openings are large enough with the same size. The goal in a dryer design process is probably not the confinement of drying air, so it is important for hot air to be able to circulate in order to remove water from the product and drive it out of the dryer. Once the air overloaded with water is out of the dryer, it requires a systematic renewal of the air without disturbing or slowing down the continuation of the drying operation, hence the uniformity of the size of the openings. This renewal and fluidity of air is ensured by these large openings of the same size.

Speaking of the optimal positions of the openings we notice that the entrance is very low while the exit very high. This can be explained by the fact that the process that governs the movement of air within a dryer greenhouse-type is natural convection. In this process, the warm air that is a little lighter will tend to rise, so move upward; this justifies the extremely high position of the exit.

Regarding the extremely low position of the inlet, it must be said that this position facilitates the implementation of the natural convection process by clearly defining the path that must

follow the overloaded air and thus avoid the slow process of air renewal, which may result in the recovery of moisture in the product to be dried.

These theoretical results seem logical and similar to those of Mujumdar [15] and Anglade and al [16] concerning the positioning of the openings of solar dryers operating in direct natural convection mode. Rakotondramiarana *and al* [17] went in the same direction as us in the context of modeling a greenhouse dryer. In fact, in this work the system to be modeled has not only uneven openings but these are also of the same dimensions so that they say, to allow natural ventilation within the greenhouse.

Student tests on temperature and air velocity when varying positions and dimensions of dryer openings; shows that there is a significant difference between the temperature and air velocity values with an α risk of 5% (Tables 1 and 2).

Let us note that the optimal size of the dryer that we have adopted, combines the interesting conditions of temperature, relative humidity and air velocity for the drying of products such as cocoa beans; according to the results of the work of Akmel [7].

4. CONCLUSION

The designed model allowed simulations; the results of the simulations gave the small dryer (h = 2,5 m and l = 3 m) with large identical openings ($l_{inlet} = l_{exit}$ = 25 cm) positioned at the two extremes: low for the inlet (Ye = 0,1 m) and high for the air outlet (Ys = 1,65 m), as energy efficient dryer ($T_{average}$ = 50,730 C). The fluidity ($V_{average}$ = 0,58 $m.s^{-1}$) of this dryer is also remarkable for the drying of agricultural products. This model unlike the others allows the control of the temperature and the velocity of the air at any point of the dryer thus allowing the efficient management and use of the dryer. It is a basic data on the operation of natural air circulation solar dryers because it takes into account the temperature and velocity gradients within the dryer.

REFERENCES

1. Kibangiou N S A. Contribution à l étude du séchage solaire de la banane plantain, de la mangue et du manioc: essais de désorption, sorption et modélisation. Thèse de doctorat, Université Felix Houphouët-Boigny, Abidjan. 2013; 230.

2. Toure S, Kibangou-Nkembo S. Chapter 463 - A Numerical Model and Experimental Study of Natural Solar Drying of Cassava in Abidjan (Cote D'Ivoire), in: Sayigh, A.A.M. (Ed.),

World Renewable Energy Congress VI. Pergamon, Oxford. 2000; 2155–2158. https://doi.org/10.1016/B978-008043865-8/50463-3.

3. Touré S, Kibangu-Nkembo S. Comparative study of natural solar drying of cassava, banana and mango. Renewable Energy. 2004; 29: 975–990. https://doi.org/10.1016/j.renene.2003.09.013.

4. Warda B. Application du séchage solaire pour la conservation des produits agro-alimentaire. Mémoire de magister, Université Kasdi Merbah Ouargla, Algérie. 2009; 149.

5. Basunia M A, Abe T. Thin-layer solar drying characteristics of rough rice under natural convection. Journal of Food Engineering. 2001; 47: 295–301. https://doi.org/10.1016/S0260-8774(00)00133-3.

6. Haoua A. Modélisation du séchage solaire sous serre des boues de stations d'épuration urbaines (These de doctorat). Université Louis Pasteur (Strasbourg). 2007; 248.

7. Akmel DC. Séchage solaire des fèves de cacao: étude expérimentale et modélisation de la cinétique de séchage. Thèse de doctorat, Université d'Abobo- Adjamé, Côte d'Ivoire. 2010; 168.

8. Liu G R, Quek S S. A non-reflecting boundary for analyzing wave propagation using the finite element method. Finite Elements in Analysis and Design. 2003; 39: 403–417. https://doi.org/10.1016/S0168-874X(02)00081-1.

9. Zienkiewicz O C, Newton R E. Coupled vibrations of a structure submerged in a compressible fluid. University of Wales, Swansea, Department of Civil Engineering, ISD, ISSC, Symposium on Finite Element Techniques at the Institut für Statik und Dynamik der luft- und Raumfahrtkonstruktionen, University of Stuttgart, Germany, Report No. C/R/101/69. 1969; 1-26.

10. Zienkiewicz O C, Taylor R L, Zhu J Z. The Finite Element Method: Its Basis and Fundamentals, in: The Finite Element Method: Its Basis and Fundamentals (Seventh Edition). Butterworth-Heinemann, Oxford. 2013; 360–378. https://doi.org/10.1016/B978-1-85617-633-0.00019-8.

11. Mitra S, Sinhamahapatra K. 2D simulation of fluid-structure interaction using finite element method. Finite Elements in Analysis and Design. 2008; 45: 52–59. https://doi.org/10.1016/j.finel.2008.07.006.

12. Battaglia J L, Kuzik A, Puiggali J R. *Introduction aux transferts thermiques*. 2e édition Dunod.; 2014.

13. Adrian B. Convection Heat Transfer. 4th Edition. John Wiley & Sons; 2013.

14. Le Quéré P. "On the computation of some external or partially enclosed natural convection flows" The 7th International Conference on Computational Heat and Mass Transfer, Istanbul, Turkey. 2011; 401_1, 401_8. hal-00619244.

15. Mujumdar A S. Handbook of Industrial Drying 2nd, Mc Gill University. Montreal, Quebec, Canada. 1987; 948.

16. Anglade A, Brunet P, Varagnat F. Pratique du séchage solaire à Koumbidia (Sénégal)., Journées Internationales de Bordeaux: : "Séchage solaire et développement rural". ed, Organisées par la cellule Energie renouvelables (GRET-GERES), Groupe de Travail TAA – GERDAT,. Laboratoire Energétique et Phénomènes de Transfert LEPT-ENSAM. 1983; 207-221.

17. Rakotondramiarana H, Morau D , Adelard L, Gatina J. Modélisation du séchage solaire: application au séchage en couche mince des boues solides des stations d'épuration. 2005.